Comparative investigation of solid electrolyte interphases created by the electrolyte additives vinyl ethylene carbonate and dicyano ketene vinyl ethylene acetal

Coralie Forestier, Piotr Jankowski, Agnieszka Wizner, Carine Davoisne, Grégory Gachot, Lucas Sannier, Sylvie Grugeon, Patrik Johansson, Michel Armand, Stéphane Laruelle

Comparative investigation of solid electrolyte interphases created by the electrolyte additives vinyl ethylene carbonate and dicyano ketene vinyl ethylene acetal

Coralie Forestier[abe], Piotr Jankowski[cd], Agnieszka Wizner[ab], Carine Davoisne[ab], Grégory Gachot[ab], Lucas Sannier[e], Sylvie Grugeon[ab], Patrik Johansson[df], Michel Armand[a], and Stephane Laruelle[ab*]

[a]*Laboratoire de Réactivité et Chimie des Solides, CNRS UMR 7314, Université de Picardie Jules Verne, 33 rue Saint Leu, 80039 Amiens, France*
[b]*Réseau sur le Stockage Electrochimique de l'Energie, CNRS RS2E FR3459, France*
[c]*Warsaw University of Technology, Faculty of Chemistry, 00-664 Warszawa, ul. Noakowskieg 3, Poland*
[d]*Department of Applied Physics, Chalmers University of Technology, SE-412 96 Gothenburg, Sweden*
[e]*Renault, DEA-IREB, Technocentre, 1 avenue du Golf, 78288 Guyancourt, France*
[f]*ALISTORE-ERI European Research Institute, 33 rue Saint Leu, 80039 Amiens, France*

[*]*corresponding author : stephane.laruelle@u-picardie.fr*
Tel : +33 322827585 Fax : +33 322827585

ABSTRACT

The effect of the replacement of the carbonyl oxygen in VEC additive by $=C(CN)_2$ in the analoguous dicyano ketene vinyl ethylene acetal (DCKVEA) on the electrochemical reduction profile is significant. Yet, the additives were proven, through IR spectroscopy supported by DFT computations, by applying EELS techniques and performing synthesis of a reduction product, to reduce in a similar way. Interestingly, the reduction-induced capacities were found to be quite different and can be explained either by the different properties of the SEI, from lithium carbonate and its malononitrile homologue, or by the different abilities of the two additives to solvate Li^+.

Keywords: Li-ion battery, SEI, additives, DFT, vinyl ethylene carbonate, dicyano ketene alkylene acetal

1. INTRODUCTION

The Li-ion battery has become the key energy storage technology to power everyday consumer goods such as laptops, mobile phones, etc. [1]. Over the last decade, with the objective of cutting emissions and reducing global warming, this technology has also been implemented in larger equipment such as electric cars to abate pollution, especially in large cities. Obviously, this emerging prospect comes with new challenges such as lifetime improvement, extremely important for a large expensive electric car battery. This has encouraged stakeholders to enhance the long-term stability of i) electrodes materials by controlling crystallographic and textural changes such as particle swelling and crystallographic phase transitions, and ii) the interphases in contact with the electrolyte by physical and chemical modifications. The simplest approach to overcome interphase-related issues is to alter the electrolyte formulation starting from the standard lithium hexafluorophosphate salt ($LiPF_6$) dissolved in a carbonate solvent mixture. The well-known solid electrolyte interphase (SEI) [2] film which is electrochemically formed at the negative electrode active material surface, as typically graphite, silicon or alkali metals, hinders the carbonate solvents reduction and was found to be imperative to proper functionality of Li-ion batteries, thus avoiding a continuous solvent consumption at low potentials *vs.* Li^+/Li°. SEI-reinforcing additives, able to be reduced prior to the solvents, were later introduced to extend, to some degree, the cycle life of the battery. Carbon-carbon unsaturated bond containing compounds such as vinylene carbonate (VC) [3–7], vinyl ethylene carbonate (VEC) [8–19], and vinyl acetate (VA) [20,21] were, due to their probability to undergo radical/anionic polymerization under reductive conditions, envisaged as potential additive candidates. In addition, organic sulfur-containing compounds such as ethylene sulfite

(ES) [22–24], 1,3-propane sultone (PS) [25–27], prop-1-ene-1,3-sultone (PES) [28], 1,3,2-dioxathiolane-2,2-dioxide (DTD) [29] and trimethylene sulfate (TMS) [30] as well as fluorinated compounds as fluoroethylene carbonate (FEC) [31–34], and 3-fluoro-1,3-propane sultone (FPS) [35] were also proposed as SEI-forming additives. These have higher reduction potentials due to the facile cleavage of the SO_3-C bond or lower LUMO due to fluorination. However, given the plethora of potential additives and electrode materials, the formulation of the most performant electrolyte is still a challenging task that requires many tests such as electrochemical impedance spectroscopy (EIS), gaseous species identification, and cycling performance analysis (discharge capacity, coulombic efficiency, charge end point capacity…) [10]. On the other hand, for three decades, many research efforts have been devoted to the understanding additive reduction mechanisms to rationally achieve better performing SEI layers. As aforesaid, lowering the LUMO level with for instance a very electronegative atom such as fluorine on the alkylene bridge was proven useful [31-35], but, spherical particles of LiF were found to be unevenly formed within the SEI [36]. On the other hand, when the O_{ester}–CH_2 bond is made weaker as in cyclic sulfonate esters i.e. propane sultone, 1,3-PS, the electrochemical cleavage occurs easily to form the sulfonate salt without gassing. Nevertheless, the SEI created presents bad coverage properties [37]. In this vein, we undertook a study on the impact of the replacement of the carbonyl group of carbonates with $C=C(CN)_2$ displaying a considerably extended conjugation capable to delocalize an additional negative charge for a facile reduction at high potentials and a stable SEI formed.

Hence, as a continuation of our previous publication highlighting the positive impact of the EC and PC homologues featuring the $C=C(CN)_2$ group [38], a comparative characterization of the SEI layers resulting from the higher potential

electrochemical reduction of polymerizable vinylene double bond containing VEC and its non-commercial counterpart dicyano ketene vinyl ethylene acetal (DCKVEA) on graphite was made, both tested as additives in classic 1 M $LiPF_6$ in the carbonate solvent based electrolytes.

2. EXPERIMENTAL

2.1 Chemicals for synthesis. For the additive, tetracyanoethylene (TCNE) was received from Alpha and urea, 3,4-dihydroxy-1-butene (>99%) were purchased from Sigma-Aldrich. For the lithium dianion, malononitrile and lithium hydride were also purchased from Sigma-Aldrich.

2.2 Differential scanning calorimetry (DSC). The DSC experiments on the additive and the lithiated graphite CMC-based electrodes were carried out on a Netzsch DSC 204F1 heat flux differential calorimeter at a heating rate of 10 K/min under a constant argon flow of 200 mL/min.

After one lithiation, the Swagelok cells (see 2.4) were disassembled in an argon-filled glove-box. The lithiated graphite CMC-based electrodes impregnated with electrolyte were introduced in DSC aluminium crucibles; they were weighed before and after loading and crimp-sealing to determine the sample mass. The lids were manually pierced just before being placed in the apparatus. To ensure reproducibility, two DSC measurements were conducted on each sample.

2.3 Fourier Transform Infra-Red (FTIR) spectroscopy of synthesized powders and SEI layers. FTIR spectra were recorded by means of a Nicolet Avatar 370DTGS spectrometer. The synthesized powders were analyzed in attenuated total reflection (ATR) mode and the delithiated graphite (Li_0C_6) powders in transmission mode through KBr pellets. After one cycle, the cells were opened in the argon-filled glove-

box, the recovered Li_0C_6 powders were rinsed three times with DMC to eliminate residual traces of both solvents and $LiPF_6$ salt, and subsequently dried in the antechamber. Pellets were made by mixing a very small amount of Li_0C_6 powder with dry KBr. The powder containing pellet mounted on the holder was prepared in the glove-box and put in a plastic bag which was opened in the N_2-purged sample chamber of the FTIR system.

2.4 Half-cell assembling and cycling. The graphite composite powder is composed of 90 wt% of artificial graphite (particle size of 26 µm (d90) and BET surface area of 6.5 m^2/g) and 10 wt% Super P carbon black. The graphite film electrode is composed of the same artificial graphite, carboxymethyl cellulose (CMC), styrene butadiene rubber (SBR), and Super P carbon black (Timcal) (94/2/2/2 wt%). The electrolytes were prepared with 1 M $LiPF_6$ in ethylene carbonate (EC) and dimethyl carbonate (DMC) (50/50, w/w), from commercial sources known as LP30® (Merck), and the additives vinyl ethylene carbonate (VEC) (Sigma Aldrich, 99% purity) and the synthesized additive at different weight percentages. A dedicated base electrolyte was prepared from 2-methyltetrahydrofuran (Sigma Aldrich anhydrous, ≥99%, inhibitor-free) and 1 M $LiPF_6$ (Aldrich, battery grade ≥ 99.99%). The Swagelok-type half-cells were assembled in an argon-filled glove-box using 10 mg composite powder or 1 cm^2 graphite electrode as working electrode, a Whatman GF/D borosilicate glass fibre separator impregnated with 150 µL of electrolyte and a lithium metal foil. Once assembled, the cells were subjected to a C/20 galvanostatic lithiation from OCV to 0.005 V *vs.* $Li^+/Li°$ (LiC_6) or lithiation/delithiation to 1.5 V *vs.* Li^+/Li^o (Li_0C_6).

2.5 Transmission electron microscopy (TEM) and electron energy loss spectroscopy (EELS). These analyses were performed using a transmission electron

microscope FEI TECNAI F20 S-TWIN fitted with a Gatan Image Filter Tridiem in post column. The measurements were carried out with a 1-1.2 eV energy resolution determined by measuring the full width at half maximum of the zero loss peak. The following conditions were used to acquire the EELS spectra: a dispersion of 0.2 eV/ch, a convergence angle of 5.8 mrad and a collection angle of 2.2 mrad. The energy loss near edge structure (ELNES) acquisitions were performed in diffraction mode. For the Li-K edge, the background was subtracted considering a first order log-polynomial law, the multiple scatterings were removed using the Fourier Log method and the energy correction with respect to the zero loss peak was done. All the energy losses given in the text have an error of +/- 0.2 eV. In an argon-filled glove-box, the synthesized lithium dianion powder and the Li_0C_6 samples were dispersed in acetonitrile and DMC respectively prior to deposition onto TEM copper grids with holey carbon. The samples were then transferred from the glove-box to the TEM without air exposure.

2.6 Hartree-Fock (HF) and density functional theory (DFT) computations. The properties of the additives were computed by two methods: HF and DFT, the latter with the M06-2X functional [39]. The DFT/M06-2x used the C-PCM [40] solvation model with parameters for water, as a good approximation of any high dielectric ($\varepsilon>20$) solvent. The 6-311++G(d,p) basis set was used as implemented in Gaussian09 [41]. HF was employed for calculations of the LUMO energies and the electron density distribution via the atoms-in-molecule (AIM) analysis scheme [42]. DFT/M06-2X was additionally used to predict reduction paths, corresponding reduction potentials, interaction energies with lithium cation(s), and vibrational frequencies to correlate to the experimental IR data. To calculate adiabatic reduction potentials E_{abs}, the thermodynamic free energy cycle shown in Scheme 1 was used -

assuming simultaneous reduction and coordination of the cation, in order to maintain electro-neutrality:

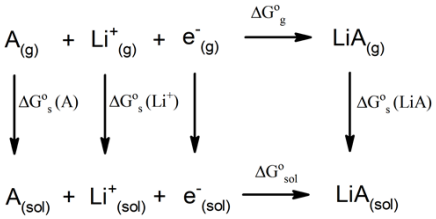

Scheme 1. Free energy cycle used for the calculation of reduction potentials.

E_{abs} (A) = $-\Delta G^{\circ}_{sol}/F = -[\Delta G^{\circ}_{gas} + \Delta G^{\circ}_{s}$ (LiA) - ΔG°_{s} (A) - ΔG°_{s} (Li^{+})]/F

where ΔG°_{sol} is the standard free energy for the reduction reaction in solution; ΔG°_{gas} is the standard free energy for the reduction reaction in the gas-phase; ΔG°_{s}(A), $\Delta G^{\circ}_{s}(Li^{+})$, and ΔG°_{s}(LiA) are the free energies of solvation of the initial compound, the lithium cation and the reduced complex, respectively. A correction of 1.46 V was used to change from absolute potentials to the Li^{+}/Li° scale [43].

3. RESULTS AND DISCUSSION

3.1 DCKVEA additive synthesis and characterization. The dicyano ketene vinyl ethylene acetal (DCKVEA) additive was synthesized following a procedure inspired by W. J. Middleton *et al.* [44]. A mixture of TCNE (2.6 mmole), urea (1.8 mmole), and 3,4-dihydroxy-1-butene (17.8 mmole) was heated up to 100°C and left under stirring for 1 hour. Then, the brownish solution was cooled prior to being poured into cold water and dichloromethane. The dichloromethane was extracted by means of a separation funnel and evaporated. The recovered material was dried under vacuum overnight at 40°C to eliminate traces of VEC that may form during the synthesis through a transdeamidification process of urea with glycol [42].

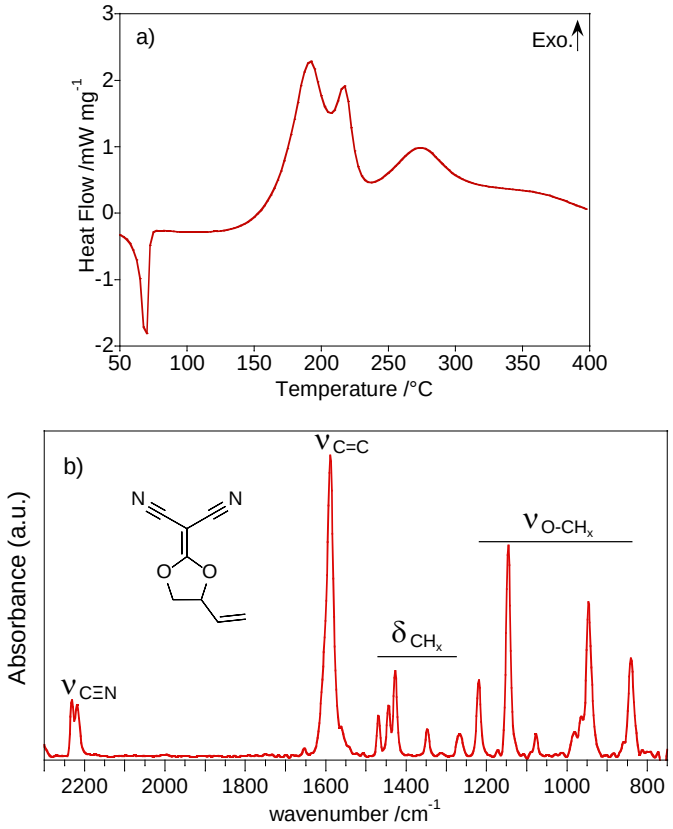

Figure 1: *a) DSC traces of and b) IR spectra of DCKVEA.*

The DSC trace of the powder displays a melting point at *ca.* 55°C (Fig. 1a) followed by exothermic peaks starting at *ca.* 150°C, attributed to its degradation and most probably to a polymerisation process through nitrile groups. The powder was then characterised by FTIR spectroscopy (Fig. 1b) with the support of DFT calculations for the assignment of the vibrational modes (Table 1). As recently found also for dicyanoketene ethylene and propylene acetals [38], DCKEA and DCKPA respectively, the spectrum shows two bands at ca. 2219 and 2232 cm^{-1} assignable to C≡N stretching vibrations. This matches well with the computed data and spectrum, providing out-of-plane and in-plane vibrations at slightly higher frequencies: 2283 and 2397 cm^{-1} and with a similar split: 14 cm^{-1} *vs.* 13 cm^{-1} experimentally. Some other features, agreeing well for computed and experimental data are gathered in the

figure in the C=C stretching, the CH_2 and CH_3 bending, and the O-CH_x stretching regions.

Assignment of DCKVEA	Wavenumbers [cm^{-1}]	
	Theoretical	Experimental
$\delta_{i.p.\ (C=)C-O}$		
$\delta_{(NC-)C=C}$	722(m)	
$\delta_{O=C}$		
$\delta_{i.p.\ (C=)C-O} + \delta_{N\equiv C-C}$	849(s)	841
$\nu_{O-C(HC2H5)}$	858(w)	
$\nu_{HC-CH2} + \nu_{HC-O}$		
$\nu_{i.p.\ O-CHx}$		
$\omega_{(C=)CH2}$	948(s)	946
$\rho_{o.o.p.\ (C=)CHx} + \nu_{i.p.\ HxC-O}$	953(s)	
$\rho_{o.o.p.\ (C=)CHx} + \nu_{o.o.p.\ HxC-O}$	972(m)	
$\tau_{o.o.p.\ (C=)CHx} + \rho_{o.o.p.\ (O-)CHx}$	985(w)	
$\nu_{HC-CH2} + \rho_{CHx}$	1007(m)	
$\nu_{HC-CH2} + \rho_{(O-)CH2}$	1061(w)	
ν_{H2C-O}		
$\nu_{(O-)C-C(=C)} + \rho_{CHx}$	1092(w)	
$\nu_{HC-O} + \nu_{(O-)HC-CH(=C)}$		
$\nu_{i.p.\ (C=)C-O} + \nu_{i.p.\ HxC-O} + \nu_{i.p.\ (N\equiv)C-C}$	1150(vs)	1148
$\nu_{o.o.p.\ (O=)C-O} + \rho_{CHx}$		
$\tau_{(O-)CH2}$	1196(s)	
$\omega_{i.p.\ (O-)CHx} + \nu_{o.o.p.\ (C=)C-O} + \nu_{o.o.p.\ (N\equiv)C-C}$	1214(s)	1219
$\omega_{i.p.\ (O-)CHx} + \delta_{C=C}$	1255(w)	
$\delta_{(C=)CHx} + \omega_{(O-)CHx}$	1263(m)	1266
$\delta_{o.o.p.\ (C=)CHx} + \omega_{i.p.\ (O-)CHx} + \nu_{o.o.p.\ HxC-O}$		
$\omega_{i.p.\ (O-)CHx}$	1323(m)	
$\omega_{o.o.p.\ (O-)CHx} + \delta_{(C=)CH2}$	1332(s)	1348
$\delta_{o.o.p.\ (C=)CHx}$	1392(m)	1427
$\omega_{i.p.\ (O-)CHx} + \nu_{o.o.p.\ (C=)C-O}$	1425(s)	1444
$\delta_{(O-)CH2}$	1460(s)	1468
$\nu_{(NC-)C=C} + \nu_{i.p.\ (C=)C-O} + \nu_{i.p.\ (N\equiv)C-C}$	1583(vs)	1589
$\nu_{H2C=CH} + \delta_{i.p.\ (C=)CHx} + \nu_{(c=)C-C(-O)}$	1668(w)	
$\nu_{O=C}$		
$\nu_{o.o.p.\ C\equiv N}$	2283(vs)	2219
$\nu_{i.p.\ C\equiv N}$	2297(s)	2232
$\nu_{C-H\ (O-CH)}$	2984(w)	
$\nu_{i.p.\ C-H\ (O-CH2)}$	3002(w)	
$\nu_{o.o.p.\ C-H\ (C=CHx)}$	3051(w)	
$\nu_{i.p.\ C-H\ (C=CHx)}$	3068(w)	
$\nu_{o.o.p.\ C-H\ (O-CH2)}$	3085(w)	
$\nu_{o.o.p.\ C-H\ (C=CH2)}$	3142(w)	

Table 1. *Theoretical and selected experimental vibrational modes for DCKVEA.*

3.2 VEC and DCKVEA reduction potential profiles. The reduction potential of DCKVEA was investigated upon the first charge of a graphite powder half-cell and compared to that of VEC. These additives were added to a LP30® electrolyte in a weight percentage as high as 5 wt% to clearly disclose their influence on the electrochemical profile. The potential *vs.* time curves (Fig. 2) unveil a quite different behavior in terms of the additive reduction potentials and consumed electrons. DCKVEA reduces between 1.9 and 1.6 V *vs.* Li^+/Li° and the charge consumed corresponds to 11% of the molar amount of the additive available considering a two-electron reduction process. In contrast, the large reduction phenomenon at *ca.* 1.3 V observed for VEC, increases this percentage to 57%. This huge difference emphasizes the more effective protective character of the SEI formed by the DCKVEA additive. In both cases, a shoulder attributed to the reduction of EC molecules is observed at *ca.* 0.8 V [45].

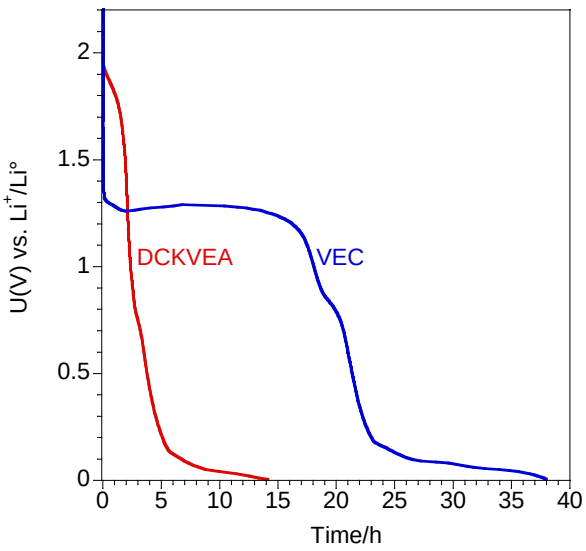

Figure 2: *Electrochemical traces of the first lithiation of graphite in LP30 electrolyte with 5 wt% of VEC or DCKVEA.*

The higher reduction ability of the dicyano ketene compound was also confirmed by the computational studies – both LUMO energies and adiabatic reduction potentials (Table 2 and 3). The energies of the LUMO for DCKVEA are 0.31 (HF) and 0.37 (DFT/M06-2X) eV lower than for VEC. The thermodynamic cycle of reduction process reveals a ca. 0.5 V difference in reduction potential between DCKVEA and VEC, in very good agreement with the experimental data (ca. 0.55 V). Detailed values depend on the chosen paths of ring-opening process (Scheme 2). Comparison of the calculated values of reduction potentials (path 1: E_{red} = 2.05 V (VEC) and 2.58 V (DCKVEA) and path 2: E_{red} = 1.49 V (VEC) and 2.04 V (DCKVEA) with experimental ones (ca. 1.3 V for VEC and starting at ca. 1.9 V for DCKVEA), suggests that the first O-C bond cleavage occurs according to the path 2 (O-CH_2 cleavage) although the calculations of reduction paths suggest path 1 to be energetically favored.

Compound	LUMO level energy [eV]	
	HF	C-PCM M06-2X
VEC	0.811	-0.001
DCKVEA	0.505	-0.371

***Table 2**: LUMO energies for VEC and DCKVEA.*

Compound	E_{red} [V vs. Li^+/Li°]	
	Path 1 O-CH bond cleavage	path 2 O-CH_2 bond cleavage
VEC	2.05	1.49
DCKVEA	2.58	2.04

***Table 3**: Adiabatic reduction potentials for VEC and DCKVEA.*

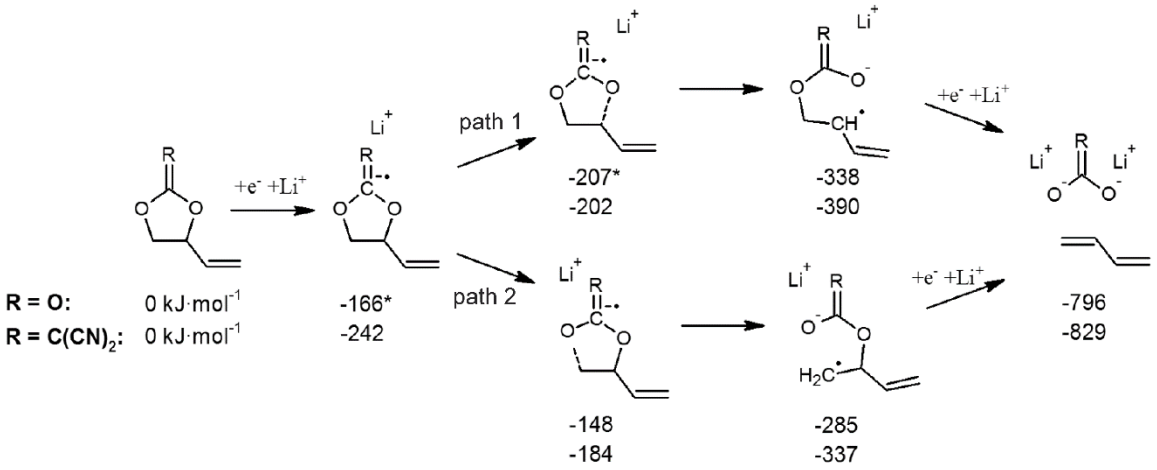

Scheme 2. Calculated mechanisms of 2-electron reduction of VEC and DCDVEA; stages marked by * were estimated by energy and gradient profile; Gibbs energies in respect to starting molecules are given in kJ·mol^{-1}.

3.3 SEI characterization and properties.

3.3.1 SEI characterization.

3.3.1.a. FTIR analysis. The significant changes in the electrochemical profiles prompt us to get further insight into the nature/composition of the resulting SEI compounds and the related reduction mechanisms. The FTIR spectra of the SEI layers formed from these 5 wt% VEC or DCKVEA containing electrolytes after one cycle are shown in Fig. 3a and 3b, respectively.

The VEC-derived SEI film spectrum reveals the presence of lithium carbonate (Li_2CO_3) as the main component with bands at ca. 1400-1500 cm^{-1} and 850 cm^{-1} of high intensity as compared to those at 1650 (CO_2 asymmetric stretching), 1300 (CH_2-CH_2 stretching), 1100 (C-O stretching) and 820 cm^{-1} (CO_3 bending) assigned to lithium alkyl carbonate salt(s) [46–48]. In addition, the GC/MS analysis of the gases recovered after the main electrolyte reduction process of a graphite/NMC111 complete cell, performed in experimental conditions described in a previous paper [49], clearly shows a peak at 30.09 min corresponding to butadiene. This result confirms previous works from Petitbon et al. [8] and Tsubouchi et al. [8] in

which a two-electron reduction mechanism is also put forward. This may be explained by the extensive conjugation of the VEC end-moiety ($CH=CH_2$) diminishing the O-CH_2 bond strength.

At this stage, after determining the layer composition, it is worth returning to the unusual VEC reduction induced extra-large plateau at 1.3 V. This specific behaviour resembles the one observed in the 1.4-1.7 potential range upon the first lithiation of a tin or bismuth (and to a lesser extent of a lead) thin film with the additive-free LP30 electrolyte [50]. The SEI layer was also found to be mainly composed of Li_2CO_3 with small amounts of lithium alkyl carbonate and direct evidences for an electrochemically-driven decomposition of EC catalysed by Sn (or Bi, or Pb) surfaces were provided. Hence, this Li_2CO_3 originating from prolonged reduction of classical carbonate based electrolytes with VEC as additive or EC as solvent does not act as a good passivating SEI layer.

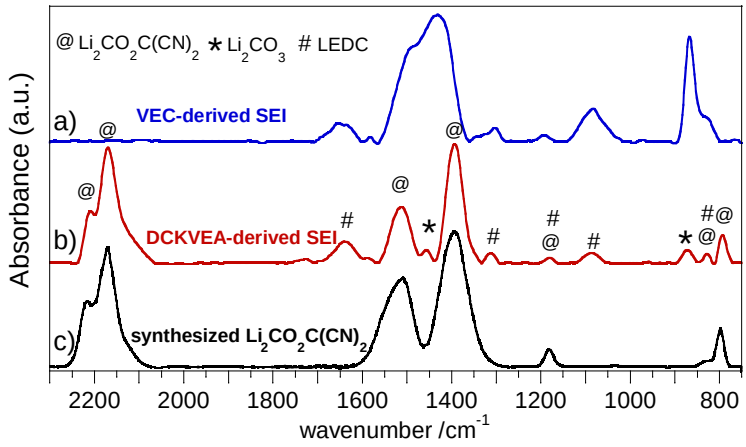

Figure 3: *a) and b) FTIR spectra of delithiated graphite powders cycled in LP30 electrolyte at a rate of C/20 with 5 wt% of VEC and DCKVEA, respectively. c) FTIR spectrum of synthesized $Li_2CO_2C(CN)_2$ reduction compound.*

The DCKVEA-derived SEI layer FTIR spectrum (Fig. 3b) reveals the presence of two stretching vibration bands related to CN groups at ca. 2170 and 2210 cm^{-1}.

These bands are slightly shifted to lower frequencies as compared to the DCKVEA: 2219 and 2232 cm^{-1} in Fig. 1. Hence, they confirm the presence of reduction product(s) in the SEI layer. When compared to those at ca. 2110, 2170 and 2210 cm^{-1} originating from the earlier studied DCKEA and DCKPA derived SEI layers [38], we note that the two bands at ca. 2170 and 2210 cm^{-1} are common and the feature at ca. 2110 cm^{-1} is missing. Comforted by the fact that also other parts of the spectra in the 700-1700 cm^{-1} region differ with characteristic bands of relatively high intensity at ca. 1512, 1385, 793 cm^{-1}, we went deeper into the SEI composition elucidation. A parallel with VEC was made by looking at the two successive steps needed to reach the foreseen "carbonate"-type $Li_2CO_2C(CN)_2$ end-product (Scheme 2 with $R=C(CN)_2$).

We synthesised this end-product (Scheme 3) in order to get reference IR data. Two equivalents of LiH were added to two equivalents of malononitrile dissolved in acetonitrile. After the formation of the malononitrile salt $(CN)_2CHLi$, 1 equivalent of malononitrile was added and the solution was left 10 min under CO_2 bubbling. After it turned into a milky-white appearance, the suspension was put into the argon-filled glove-box, centrifuged, and the recovered powder washed several times with acetonitrile and then dried.

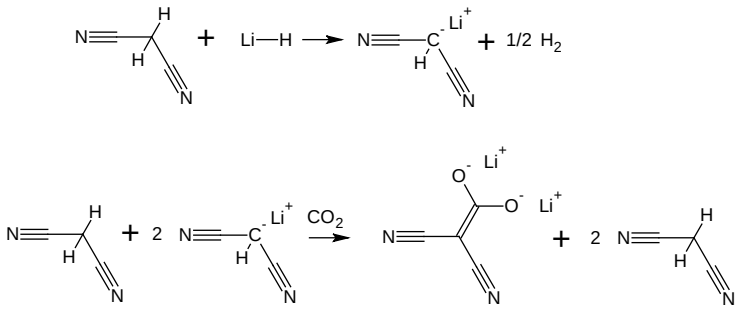

Scheme 3: Synthesis of the foreseen "carbonate"-type $Li_2CO_2C(CN)_2$ end-product.

The IR spectrum (Fig. 3c) of the product shows a few bands at ca. 2210, 2170, 1512, 1385, 1182, 879 and 793 cm^{-1} which match pretty well with those deduced from the DFT calculations (Table 4). When comparing with the DCKVEA-derived SEI spectra (Fig. 3b), we can clearly state that the SEI layer is indeed mainly composed of the "carbonate"-type ion $Li_2CO_2C(CN)_2$, confirming our hypothesis of an analogy with VEC. This is also corroborated by both EELS (below) and the detection of butadiene gas through GC/MS analysis. Other bands of weaker intensity are also observed and can be assigned to lithium alkyl carbonate salt(s) and Li_2CO_3 from EC reduction. A comparison of the two-electron reduction paths for VEC and DCKVEA are reported in Scheme 2 along with the calculated energies.

Assignment of $Li_2CO_2C(CN)_2$	Wavenumbers [cm^{-1}]	
	Theoretical	Experimental
$\delta_{C=C}$	762(s)	793
$\nu_{i.p.\ (C=)C-O} + \nu_{i.p.\ (N\equiv)C-C}$	832(s)	879
$\nu_{C=C} + \nu_{i.p.\ (N\equiv)C-C}$	1173(w)	1182
$\nu_{o.o.p.\ (N\equiv)C-C}$	1261(w)	
$\nu_{C=C} + \nu_{i.p.\ (C=)C-O}$	1341(vs)	1385
$\nu_{o.o.p.\ C-O}$	1515(vs)	1512
$\nu_{o.o.p.\ C\equiv N}$	2175(vs)	2170
$\nu_{i.p.\ C\equiv N}$	2225(vs)	2210

Table 4: *Theoretical and selected experimental vibrational modes for $Li_2CO_2C(CN)_2$.*

The synthesis of the reduction product allows us to confirm the two-electron reduction pathway for DCKVEA. Moreover, the presence of the supplementary band at ca. 2110 cm^{-1} in case of the DCKEA and DCKPA SEI layers [35] indicates the

existence of another reduction compound. This suggests that these latter additives undergo both the one and two-electron reduction pathways. Therefore, the three additives together seem to behave similarly to their carbonate counterparts VEC, EC and PC, suggesting that the replacement of the carbonyl group by the highly conjugated $C=C(CN)_2$ does not affect the reduction mechanism. However, the resulting reduction product offers different passivation properties.

3.3.1.b. TEM-EELS analysis. Here, we compare the SEIs resulting from VEC and DCKVEA mainly through ex situ analysis of texture/thickness after the samples have undergone a washing procedure. These studies were performed with a powder electrode and a LP30 electrolyte containing 2 wt% of additive to be closer to the classical percentage of many earlier studies.

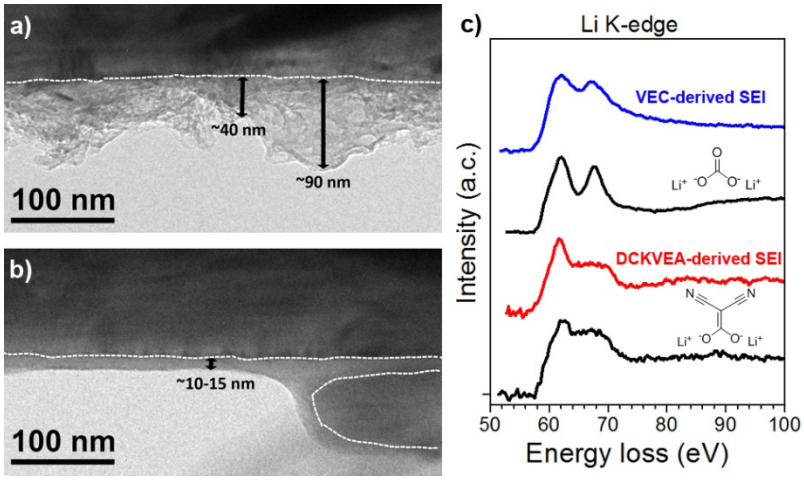

Figure 4: *a) and b) Ex situ TEM images of DMC-washed graphite SEIs after first lithiation with a LP30 electrolyte containing 2 wt% of VEC and DCKVEA, respectively. c) EELS spectra on the Li K-edge of the references $Li_2CO_2C(CN)_2$ and Li_2CO_3 (black from bottom to top), the DCKVEA-derived SEI (red) and the VEC-derived SEI (blue).*

As already revealed by some of us, via an analysis of TEM images [36], the SEI formed by VEC reduction shows, after washing, large irregularities with a thickness ranging from 40 to 90 nm (Fig. 4a). The EELS analyses on the Li K-edge

performed on this VEC-derived SEI (Fig. 4c-blue curve) show a spectrum composed of two peaks at 62.1 eV and 67.4 eV, in good agreement with those at 62.1 eV and 67.6 eV for the lithium carbonate reference [51,52]. The peak broadening observed for the VEC-derived SEI indicates the presence of other carbonates containing lithium, as also revealed by IR (Fig. 3a).

In contrast, for DCKVEA the entire surface of the graphite and the conductive carbon is perfectly covered by a smooth and uniform 10-15 nm thick SEI layer (Fig. 4b). The EELS analyses on the Li K-edge performed on the DCKVEA-derived SEI (Fig. 4c-red curve) show a spectrum composed of one sharp peak at 61.8 eV followed by a broader contribution at higher energy loss. The shape and position are both in accordance with the reference of synthesized “carbonate”-type $Li_2CO_2C(CN)_2$ (Fig. 4c), with a principal peak at 61.8 eV followed by a broader part at higher energy loss. For these two cases, DCKVEA-derived SEI and $Li_2CO_2C(CN)_2$, a contribution is also observed in the N K-edge (not shown here) confirming the presence of nitrogen-based compounds. These observations are coherent with the results obtained by IR (Fig 3b). It is interesting to note that though the SEI layers underwent a washing procedure, the textures remain very different and it is likely that the irregular Li_2CO_3 texture is responsible for its non-passivating property against further reduction of VEC.

3.3.2 SEI properties.

3.3.2.a. GC/MS analysis. As demonstrated in previous studies [37], monitoring of bis-carbonate molecules stemming from the electrochemical reduction of linear carbonate solvents, at ca. 0.8 V, is an elegant way to prove the passivation properties of the SEI layers formed. On this basis, the electrolytes recovered from the Swagelok cells containing graphite powder/NMC111, charged at room temperature

up to 4.15 V, were analyzed according to the same protocol described by H. Kim *et al.* [37]. Through liquid GC/MS, the bis-carbonate molecule (dimethyl 2,5-dioxahexane dicarboxylate (DMDOHC)) was tracked, appearing at ca. 18.3 min in the chromatogram. Without any additive (Fig. 5a), the relative signal intensity of DMDOHC is ca. 17% *vs.* EC (2 mol% *vs.* EC), close to the maximum of ca. 23% reported by H. Kim et al.. With 2 wt% of DCKVEA added, no traces of DMDOHC were detected (Fig. 5b). It is worth mentioning that the mass spectrum relative to the very weak peak (0.5% intensity vs. EC signal) observed at 18.49 min does not correspond to the DMDOHC molecule (Fig. 5c) but to the DCKVEA additive (Fig. 5d). The absence of soluble degradation compound reflects the good passivation properties of the DCKVEA-derived SEI layer as also pointed out above by the fact that it evenly covers the graphite particles surface.

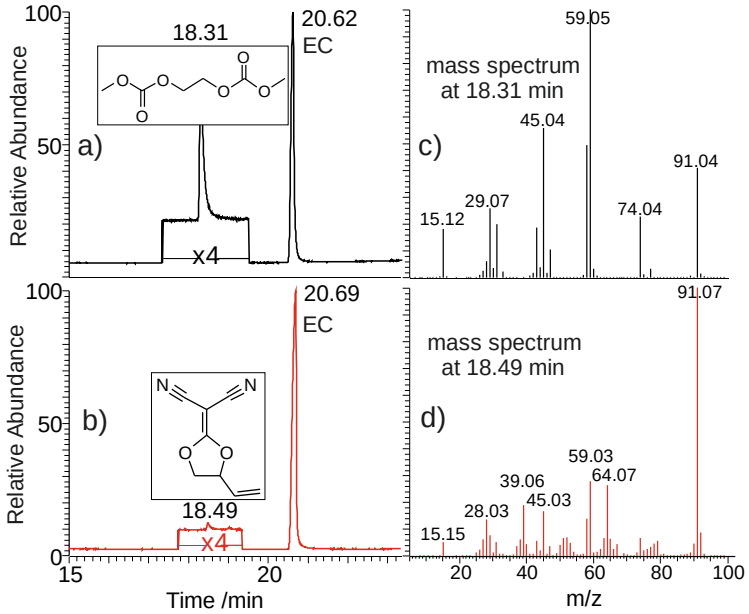

Figure 5: *Liquid GC/MS chromatograms of the electrolyte after 1 lithiation at 20°C in LP30 electrolyte a) without and b) with 2 wt% DCKVEA added. c) and d) corresponding mass spectra of the peak at 18.31 and 18.40 min, respectively.*

The relative signal intensity of the DMDOHC was reported [37] to be very weak for VEC 2 wt%-based electrolytes, ca. 1.1 % *vs.* the EC signal. This means that the Li_2CO_3-based SEI offers better passivation properties than the SEI formed using an additive-free electrolyte containing lithium alkyl carbonate(s). However, this is at odds with the occurrence of a long reduction plateau at ca. 1.3 V for the VEC 5 wt%-based electrolyte (Fig. 2). Such a Li_2CO_3-based SEI layer behavior seems unconventional as it suggests that passage of VEC or even EC (as discussed with respect to catalytic support) through the SEI layer is not hindered, to allow their reduction at high potential. These VEC and EC molecules display a similar charges distribution from AIM analysis (Table 5) and probably similar donor numbers (the DN of EC is 16.4) as their interaction energies with a lithium cation are similar: 18.5 and 17.1 $kJ \cdot mol^{-1}$, respectively. Therefore, Li^+-VEC (or EC) can be driven through the Li_2CO_3 SEI layer under the influence of an electric field.

3.3.2.b. Solvent influence. The aforementioned hypothesis is supported by supplementary graphite lithiation experiments in the presence of 5 wt% VEC or DCKVEA wherein EC and DMC carbonates solvents were replaced by MeTHF. This solvent has a stronger interaction with Li^+ (25.5 $kJ \cdot mol^{-1}$) and thus a higher DN, the DN of THF being 20. As shown in Fig. 6, the change in solvent does not affect the DCKVEA reduction behavior at ca. 1.8 V; only the EC reduction-derived shoulder at 0.8 V has obviously disappeared. In contrast, the long plateau pertaining to VEC reduction at ca. 1.3 V has considerably decreased; only a small plateau at ca. 1.4 V of roughly the same capacity as for DCKVEA is observed. If MeTHF indeed interacts stronger with Li^+ than VEC, the latter is then less prone to go through the SEI to be reduced, hence limiting the length of the plateau. Furthermore, the replacement of C=O by $C=C(CN)_2$ impacts the charge distribution (Table 5). As $=C(CN)_2$ is a weaker

electron withdrawing group than =O, it has less propensity to solvate Li^+, which explains why the reduction behaviour of DCKVEA does not change as a function of the solvent.

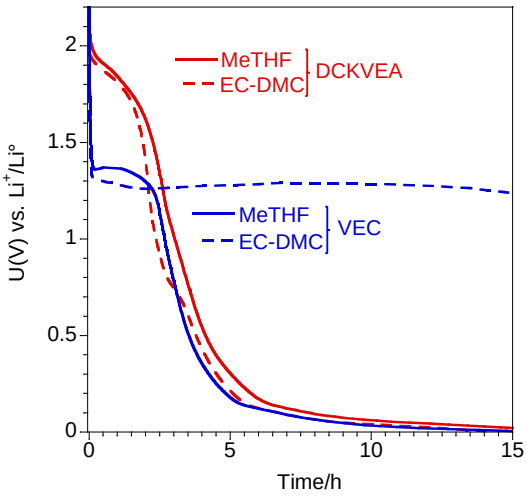

Figure 6: *Electrochemical traces of the first lithiation of graphite in LP30 or MeTHF/1M $LiPF_6$ with 5 wt% of VEC or DCKVEA.*

	HF			C-PCM M06-2X		
	EC	VEC	DCKVEA	EC	VEC	DCKVEA
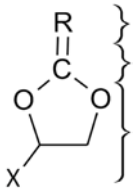	-1.35	-1.35	-0.13	-1.22	-1.22	-0.38
	+2.59	+2.60	+1.35	+2.23	+2.23	+1.34
	-1.26	-1.25	-1.22	-1.01	-1.01	-0.96

Table 5

Table 5: *AIM analysis of charge distribution in VEC and DCKVEA molecules.*

3.3.2.c. DSC analysis. The DSC profile of the heat flow generated upon heating any LiC_6/electrolyte system depends on the SEI composition and texture [36]. DSC measurements on CMC-based graphite electrodes, recovered after one lithiation in VEC or DCKVEA 0.5 wt% containing LP30 electrolyte, were made to

compare the influence of the Li_2CO_3 and $Li_2CO_2C(CN)_2$ based SEI layers. The experiments, carried out on film electrodes, proved to provide highly reproducible heat flow profiles and an additive content as low as 0.5 wt% for the $C(CN)_2$ moiety was shown to have a beneficial effect on the capacity retention for the small Li-ion battery pouch cells. From the DSC traces (Fig. 7), similar enthalpies, ca. 620±25 J/g, were obtained without and with additives, but the exothermic shoulder at 130-150°C related to SEI breakdown differs in intensity. The slightly higher intensity for VEC is in agreement with a SEI breakdown mostly triggered by an exothermic acid-base reaction between Li_2CO_3 and PF_5 [53]. In contrast, the shoulder is less pronounced with DCKVEA, explainable by the weaker electron withdrawing effect of the $=C(CN)_2$ group making $Li_2CO_2C(CN)_2$ less basic than Li_2CO_3 and therefore less reactive towards PF_5.

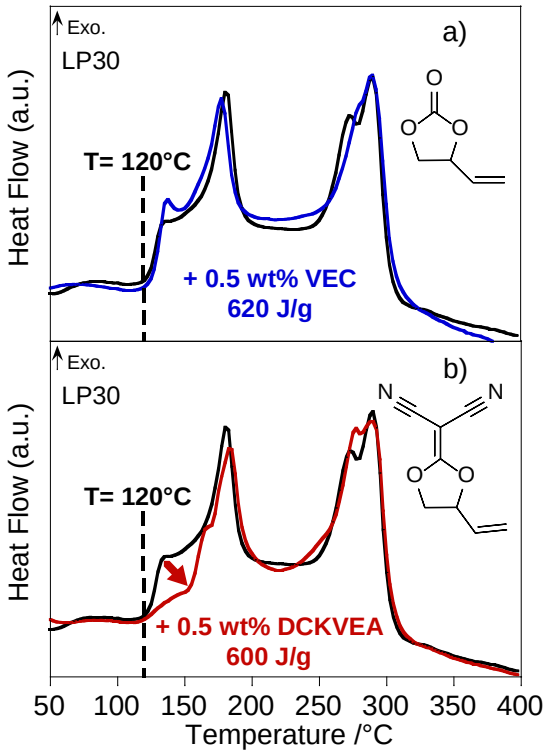

Figure 7: *DSC profiles of lithiated graphite film/electrolyte cycled at a rate of C/20 in LP30 electrolyte with 0.5 wt% of a) VEC and b) DCKVEA.*

CONCLUSION

The vinyl ethylene group based additives VEC and the herein synthesized DCKVEA were found to reduce on a graphite powder composite at ca. 1.3 and 1.8 V *vs.* Li/Li^+, respectively, and this was supported by DFT calculations of their reduction potentials.

A thorough characterization was made of the resulting SEI layers by IR spectroscopy supported by DFT computations and EELS techniques. A comparison of the lithium carbonate and the successfully synthesized pseudo "lithium carbonate" $Li_2CO_2C(CN)_2$, demonstrated that both VEC and DCKVEA are prone to a two-electron reductive cleavage. More generally, the replacement of the carbonyl group of VEC, EC, and PC carbonates by $C=C(CN)_2$ does not impact the reduction mechanisms of the additives, but modifies the properties of the resulting SEI layers.

The quite much larger reduction-induced capacity of VEC as compared to DCKVEA, when added at relatively high concentrations in carbonate-based electrolytes, was unforeseen. The long plateau bears resemblance to the one of catalytic supports (Bi, Sn or Pb) for two-electron reduction of EC in the 1.4-1.7 V range, leading to a thick layer of lithium carbonate. The lithium carbonate inhomogeneous layer formed from VEC or EC (on catalytic support for the latter) was found not to be a good passivation layer towards the permeation of Li^+-molecule solvates. In analogy, we here show that the electrolyte solvents could impact on the reduction-induced capacity of VEC. Replacing EC and DMC solvents with a solvent having a higher donor number, MeTHF, should decrease the probability for VEC to solvate Li^+ and thereby its permeation across the SEI to reduce, and a shortening of the reduction plateau of VEC is indeed obtained. Unlike VEC, DCKVEA does not

present a long reduction plateau, which can be explained either by a better film-forming property of the $Li_2CO_2C(CN)_2$ layer and/or by less propensity to solvate Li^+.

ACKNOWLEDGMENT

Support from the Association Nationale de la Recherche et de la Technologie (ANRT, France) is gratefully acknowledged. Calculations have been carried out at the Wroclaw Centre for Networking and Supercomputing (http://www.wcss.pl), grant No. 346. The support by Chalmers Area of Advance Energy for a travel scholarship to Piotr Jankowski is gratefully acknowledged. Patrik Johansson acknowledges both the Swedish Energy Agency for a basic research grant via the Swedish Research Council and the continuous support by many of Chalmers Areas of Advance: Energy, Materials Science, and Transport. We also thank Carine Lenfant for proofreading this paper.

References

[1] R. Wagner, N. Preschitschek, S. Passerini, J. Leker, M. Winter, Current research trends and prospects among the various materials and designs used in lithium-based batteries, J. Appl. Electrochem. 43 (2013) 481–496. doi:10.1007/s10800-013-0533-6.

[2] E. Peled, The Electrochemical Behavior of Alkali and Alkaline Earth Metals in Nonaqueous Battery Systems—The Solid Electrolyte Interphase Model, J. Electrochem. Soc. 126 (1979) 2047–2051. doi:10.1149/1.2128859.

[3] H. Ota, Y. Sakata, A. Inoue, S. Yamaguchi, Analysis of Vinylene Carbonate Derived SEI Layers on Graphite Anode, J. Electrochem. Soc. 151 (2004) A1659–A1669. doi:10.1149/1.1785795.

[4] M. Nie, J. Demeaux, B.T. Young, D.R. Heskett, Y. Chen, A. Bose, J.C. Woicik, B.L. Lucht, Effect of Vinylene Carbonate and Fluoroethylene Carbonate on SEI Formation on Graphitic Anodes in Li-Ion Batteries, J. Electrochem. Soc. 162 (2015) A7008–A7014. doi:10.1149/2.0021513jes.

[5] D. Aurbach, K. Gamolsky, B. Markovsky, Y. Gofer, M. Schmidt, U. Heider, On the use of vinylene carbonate (VC) electrolyte solutions for Li-ion as an additive to batteries, Electrochimica Acta. 47 (2002) 1423–1439. doi:10.1016/S0013-4686(01)00858-1.

[6] L.E. Ouatani, R. Dedryvère, C. Siret, P. Biensan, S. Reynaud, P. Iratçabal, D. Gonbeau, The Effect of Vinylene Carbonate Additive on Surface Film Formation on Both Electrodes in Li-Ion Batteries, J. Electrochem. Soc. 156 (2009) A103–A113. doi:10.1149/1.3029674.

[7] R.D. Deshpande, P. Ridgway, Y. Fu, W. Zhang, J. Cai, V. Battaglia, The Limited Effect of VC in Graphite/NMC Cells, J. Electrochem. Soc. 162 (2015) A330–A338. doi:10.1149/2.0221503jes.

[8] R. Petibon, E.C. Henry, J.C. Burns, N.N. Sinha, J.R. Dahn, Comparative Study of Vinyl Ethylene Carbonate (VEC) and Vinylene Carbonate (VC) in LiCoO2/Graphite Pouch Cells Using High Precision Coulometry and Electrochemical Impedance Spectroscopy Measurements on Symmetric Cells, J. Electrochem. Soc. 161 (2014) A66–A74. doi:10.1149/2.030401jes.

[9] S. Tsubouchi, Y. Domi, T. Doi, M. Ochida, H. Nakagawa, T. Yamanaka, T. Abe, Z. Ogumi, Spectroscopic Characterization of Surface Films Formed on Edge Plane Graphite in Ethylene Carbonate-Based Electrolytes Containing Film-Forming Additives, J. Electrochem. Soc. 159 (2012) A1786–A1790. doi:10.1149/2.028211jes.

[10] D.Y. Wang, N.N. Sinha, J.C. Burns, R. Petibon, J.R. Dahn, A high precision study of the electrolyte additives vinylene carbonate, vinyl ethylene carbonate and lithium bis(oxalate)borate in LiCoO2/graphite pouch cells, J. Power Sources. 270 (2014) 68–78. doi:10.1016/j.jpowsour.2014.07.053.

[11] J. Li, W. Yao, Y.S. Meng, Y. Yang, Effects of Vinyl Ethylene Carbonate Additive on Elevated-Temperature Performance of Cathode Material in Lithium Ion Batteries, J. Phys. Chem. C. 112 (2008) 12550–12556. doi:10.1021/jp800336n.

[12] Y. Hu, W. Kong, H. Li, X. Huang, L. Chen, Experimental and theoretical studies on reduction mechanism of vinyl ethylene carbonate on graphite anode for lithium ion batteries, Electrochem. Commun. 6 (2004) 126–131. doi:10.1016/j.elecom.2003.10.024.

[13] X. Zuo, J. Wu, M. Zhao, C. Wang, J. Liu, J. Nan, Vinyl ethylene carbonate as an electrolyte additive for high-voltage LiNi0.4Mn0.4Co0.2O2/graphite Li-ion batteries, Ionics. 22 (2015) 201–208. doi:10.1007/s11581-015-1536-6.

[14] Y. Domi, M. Ochida, S. Tsubouchi, H. Nakagawa, T. Yamanaka, T. Doi, T. Abe, Z. Ogumi, Electrochemical AFM Observation of the HOPG Edge Plane in Ethylene Carbonate-Based Electrolytes Containing Film-Forming Additives, J. Electrochem. Soc. 159 (2012) A1292–A1297. doi:10.1149/2.059208jes.

[15] S.-H. Lee, I.-S. Jo, J. Kim, Surface analysis of the solid electrolyte interface formed by additives on graphite electrodes in Li-ion batteries using XPS, FE-AES, and XHR-SEM techniques, Surf. Interface Anal. 46 (2014) 570–576. doi:10.1002/sia.5575.

[16] M.C. Smart, B.L. Lucht, B.V. Ratnakumar, Electrochemical Characteristics of MCMB and LiNi x Co1 − x O2 Electrodes in Electrolytes with Stabilizing Additives, J. Electrochem. Soc. 155 (2008) A557–A568. doi:10.1149/1.2928611.
[17] J. Liu, Z. Chen, S. Busking, I. Belharouak, K. Amine, Effect of electrolyte additives in improving the cycle and calendar life of graphite/Li1.1[Ni1/3Co1/3Mn1/3]0.9O2 Li-ion cells, J. Power Sources. 174 (2007) 852–855. doi:10.1016/j.jpowsour.2007.06.225.
[18] R. Wang, X. Li, Z. Wang, H. Guo, J. Wang, T. Hou, Impacts of vinyl ethylene carbonate and vinylene carbonate on lithium manganese oxide spinel cathode at elevated temperature, J. Alloys Compd. 632 (2015) 435–444. doi:10.1016/j.jallcom.2015.01.220.
[19] D.Y. Wang, N.N. Sinha, R. Petibon, J.C. Burns, J.R. Dahn, A systematic study of well-known electrolyte additives in LiCoO2/graphite pouch cells, J. Power Sources. 251 (2014) 311–318. doi:10.1016/j.jpowsour.2013.11.064.
[20] K. Abe, H. Yoshitake, T. Kitakura, T. Hattori, H. Wang, M. Yoshio, Additives-containing functional electrolytes for suppressing electrolyte decomposition in lithium-ion batteries, Electrochimica Acta. 49 (2004) 4613–4622. doi:10.1016/j.electacta.2004.05.016.
[21] K. Abe, K. Miyoshi, T. Hattori, Y. Ushigoe, H. Yoshitake, Functional electrolytes: Synergetic effect of electrolyte additives for lithium-ion battery, J. Power Sources. 184 (2008) 449–455. doi:10.1016/j.jpowsour.2008.03.037.
[22] G.H. Wrodnigg, J.O. Besenhard, M. Winter, Ethylene Sulfite as Electrolyte Additive for Lithium-Ion Cells with Graphitic Anodes, J. Electrochem. Soc. 146 (1999) 470–472. doi:10.1149/1.1391630.
[23] G.H. Wrodnigg, T.M. Wrodnigg, J.O. Besenhard, M. Winter, Propylene sulfite as film-forming electrolyte additive in lithium ion batteries, Electrochem. Commun. 1 (1999) 148–150. doi:10.1016/S1388-2481(99)00023-5.
[24] G.H. Wrodnigg, J.O. Besenhard, M. Winter, Ethylene Sulfite as Electrolyte Additive for Lithium-Ion Cells with Graphitic Anodes, J. Electrochem. Soc. 146 (1999) 470–472. doi:10.1149/1.1391630.
[25] J. Pires, L. Timperman, A. Castets, J.S. Peña, E. Dumont, S. Levasseur, R. Dedryvère, C. Tessier, M. Anouti, Role of propane sultone as an additive to improve the performance of a lithium-rich cathode material at a high potential, RSC Adv. 5 (2015) 42088–42094. doi:10.1039/C5RA05650K.
[26] M. Xu, W. Li, B.L. Lucht, Effect of propane sultone on elevated temperature performance of anode and cathode materials in lithium-ion batteries, J. Power Sources. 193 (2009) 804–809. doi:10.1016/j.jpowsour.2009.03.067.
[27] X. Zuo, M. Xu, W. Li, D. Su, J. Liu, Electrochemical Reduction of 1,3-Propane Sultone on Graphite Electrodes and Its Application in Li-Ion Batteries, Electrochem. Solid-State Lett. 9 (2006) A196–A199. doi:10.1149/1.2170462.
[28] B. Li, M. Xu, B. Li, Y. Liu, L. Yang, W. Li, S. Hu, Properties of solid electrolyte interphase formed by prop-1-ene-1,3-sultone on graphite anode of Li-ion batteries, Electrochimica Acta. 105 (2013) 1–6. doi:10.1016/j.electacta.2013.04.142.
[29] L. Madec, J. Xia, R. Petibon, K.J. Nelson, J.-P. Sun, I.G. Hill, J.R. Dahn, Effect of Sulfate Electrolyte Additives on LiNi1/3Mn1/3Co1/3O2/Graphite Pouch Cell Lifetime: Correlation between XPS Surface Studies and Electrochemical Test Results, J. Phys. Chem. C. 118 (2014) 29608–29622. doi:10.1021/jp509731y.
[30] Felix, J.-H. Cheng, S. Hy, J. Rick, F.-M. Wang, B.-J. Hwang, Mechanistic Basis of Enhanced Capacity Retention Found with Novel Sulfate-Based Additive in High-Voltage Li-Ion Batteries, J. Phys. Chem. C. 117 (2013) 22619–22626. doi:10.1021/jp409779x.
[31] R. McMillan, H. Slegr, Z.X. Shu, W. Wang, Fluoroethylene carbonate electrolyte and its use in lithium ion batteries with graphite anodes, J. Power Sources. 81–82 (1999) 20–26. doi:10.1016/S0378-7753(98)00201-8.
[32] N.-S. Choi, K.H. Yew, K.Y. Lee, M. Sung, H. Kim, S.-S. Kim, Effect of fluoroethylene carbonate additive on interfacial properties of silicon thin-film electrode, J. Power Sources. 161 (2006) 1254–1259. doi:10.1016/j.jpowsour.2006.05.049.

[33] H. Shin, J. Park, A.M. Sastry, W. Lu, Effects of Fluoroethylene Carbonate (FEC) on Anode and Cathode Interfaces at Elevated Temperatures, J. Electrochem. Soc. 162 (2015) A1683–A1692. doi:10.1149/2.0071509jes.
[34] Y. Lee, J. Lee, H. Kim, K. Kang, N.-S. Choi, Highly stable linear carbonate-containing electrolytes with fluoroethylene carbonate for high-performance cathodes in sodium-ion batteries, J. Power Sources. 320 (2016) 49–58. doi:10.1016/j.jpowsour.2016.04.070.
[35] H.M. Jung, S.-H. Park, J. Jeon, Y. Choi, S. Yoon, J.-J. Cho, S. Oh, S. Kang, Y.-K. Han, H. Lee, Fluoropropane sultone as an SEI-forming additive that outperforms vinylene carbonate, J. Mater. Chem. A. 1 (2013) 11975–11981. doi:10.1039/C3TA12580G.
[36] C. Forestier, S. Grugeon, C. Davoisne, A. Lecocq, G. Marlair, M. Armand, L. Sannier, S. Laruelle, Graphite electrode thermal behavior and solid electrolyte interphase investigations: Role of state-of-the-art binders, carbonate additives and lithium bis(fluorosulfonyl)imide salt, J. Power Sources. 330 (2016) 186–194. doi:10.1016/j.jpowsour.2016.09.005.
[37] H. Kim, S. Grugeon, G. Gachot, M. Armand, L. Sannier, S. Laruelle, Ethylene bis-carbonates as telltales of SEI and electrolyte health, role of carbonate type and new additives, Electrochimica Acta. 136 (2014) 157–165. doi:10.1016/j.electacta.2014.05.072.
[38] C. Forestier, P. Jankowski, L. Coser, G. Gachot, L. Sannier, P. Johansson, M. Armand, S. Grugeon, S. Laruelle, Facile reduction of pseudo-carbonates: Promoting solid electrolyte interphases with dicyanoketene alkylene acetals in lithium-ion batteries, J. Power Sources. 303 (2016) 1–9. doi:10.1016/j.jpowsour.2015.10.103.
[39] Y. Zhao, D.G. Truhlar, The M06 suite of density functionals for main group thermochemistry, thermochemical kinetics, noncovalent interactions, excited states, and transition elements: two new functionals and systematic testing of four M06-class functionals and 12 other functionals, Theor. Chem. Acc. 120 (2007) 215–241. doi:10.1007/s00214-007-0310-x.
[40] V. Barone, M. Cossi, Quantum Calculation of Molecular Energies and Energy Gradients in Solution by a Conductor Solvent Model, J. Phys. Chem. A. 102 (1998) 1995–2001. doi:10.1021/jp9716997.
[41] Gaussian 09, Revision E.01, M. J. Frisch, G. W. Trucks, H. B. Schlegel, G. E. Scuseria, M. A. Robb, J. R. Cheeseman, G. Scalmani, V. Barone, B. Mennucci, G. A. Petersson, H. Nakatsuji, M. Caricato, X. Li, H. P. Hratchian, A. F. Izmaylov, J. Bloino, G. Zheng, J. L. Sonnenberg, M. Hada, M. Ehara, K. Toyota, R. Fukuda, J. Hasegawa, M. Ishida, T. Nakajima, Y. Honda, O. Kitao, H. Nakai, T. Vreven, J. A. Montgomery, Jr., J. E. Peralta, F. Ogliaro, M. Bearpark, J. J. Heyd, E. Brothers, K. N. Kudin, V. N. Staroverov, R. Kobayashi, J. Normand, K. Raghavachari, A. Rendell, J. C. Burant, S. S. Iyengar, J. Tomasi, M. Cossi, N. Rega, J. M. Millam, M. Klene, J. E. Knox, J. B. Cross, V. Bakken, C. Adamo, J. Jaramillo, R. Gomperts, R. E. Stratmann, O. Yazyev, A. J. Austin, R. Cammi, C. Pomelli, J. W. Ochterski, R. L. Martin, K. Morokuma, V. G. Zakrzewski, G. A. Voth, P. Salvador, J. J. Dannenberg, S. Dapprich, A. D. Daniels, Ö. Farkas, J. B. Foresman, J. V. Ortiz, J. Cioslowski, and D. J. Fox, Gaussian, Inc., Wallingford CT, 2009.
[42] R.F.W. Bader, Atoms in Molecules: A Quantum Theory, 1st Paperback Edition edition, Clarendon Press, 1994.
[43] S. Trasatti, The absolute electrode potential: an explanatory note (Recommendations 1986), Pure Appl. Chem. 58 (1986). doi:10.1351/pac198658070955.
[44] W.J. Middleton, V.A. Engelhardt, Cyanocarbon Chemistry. IV.1 Dicyanoketene Acetals, J. Am. Chem. Soc. 80 (1958) 2788–2795. doi:10.1021/ja01544a054.
[45] A. Naji, J. Ghanbaja, P. Willmann, B. Humbert, D. Billaud, First characterization of the surface compounds formed during the reduction of a carbonaceous electrode in LiClO4-ethylene carbonate electrolyte, J. Power Sources. 62 (1996) 141–143. doi:10.1016/S0378-7753(96)02401-9.
[46] D. Aurbach, B. Markovsky, I. Weissman, E. Levi, Y. Ein-Eli, On the correlation between surface chemistry and performance of graphite negative electrodes for Li ion batteries, Electrochimica Acta. 45 (1999) 67–86. doi:10.1016/S0013-4686(99)00194-2.

[47] K. Xu, G.R.V. Zhuang, J.L. Allen, U. Lee, S.S. Zhang, P.N. Ross, T.R. Jow, Syntheses and characterization of lithium alkyl mono- and dicarbonates as components of surface films in Li-Ion batteries, J. Phys. Chem. B. 110 (2006) 7708–7719. doi:10.1021/jp0601522.
[48] L. Gireaud, S. Grugeon, S. Laruelle, S. Pilard, J.M. Tarascon, Identification of Li Battery Electrolyte Degradation Products Through Direct Synthesis and Characterization of Alkyl Carbonate Salts, J. Electrochem. Soc. 152 (2005) A850–A857. doi:10.1149/1.1872673.
[49] G. Gachot, S. Grugeon, I. Jimenez-Gordon, G.G. Eshetu, S. Boyanov, A. Lecocq, G. Marlair, S. Pilard, S. Laruelle, Gas chromatography/Fourier transform infrared/mass spectrometry coupling: a tool for Li-ion battery safety field investigation, Anal. Methods. (2014). doi:10.1039/C4AY00054D.
[50] J.-S. Bridel, S. Grugeon, S. Laruelle, J. Hassoun, P. Reale, B. Scrosati, J.-M. Tarascon, Decomposition of ethylene carbonate on electrodeposited metal thin film anode, J. Power Sources. 195 (2010) 2036–2043. doi:10.1016/j.jpowsour.2009.10.038.
[51] F. Cosandey, D. Su, M. Sina, N. Pereira, G.G. Amatucci, Fe valence determination and Li elemental distribution in lithiated FeO0.7F1.3/C nanocomposite battery materials by electron energy loss spectroscopy (EELS), Micron. 43 (2012) 22–29. doi:10.1016/j.micron.2011.05.009.
[52] F. Wang, J. Graetz, M.S. Moreno, C. Ma, L. Wu, V. Volkov, Y. Zhu, Chemical Distribution and Bonding of Lithium in Intercalated Graphite: Identification with Optimized Electron Energy Loss Spectroscopy, ACS Nano. 5 (2011) 1190–1197. doi:10.1021/nn1028168.
[53] G.G. Eshetu, S. Grugeon, G. Gachot, D. Mathiron, M. Armand, S. Laruelle, LiFSI vs. LiPF6 electrolytes in contact with lithiated graphite: Comparing thermal stabilities and identification of specific SEI-reinforcing additives, Electrochimica Acta. 102 (2013) 133–141. doi:10.1016/j.electacta.2013.03.171.